



HHS Public Access

Author manuscript

Nat Med. Author manuscript; available in PMC 2010 May 04.

Published in final edited form as:

Nat Med. 2009 February ; 15(2): 159–168. doi:10.1038/nm.1904.

AdPLA ablation increases lipolysis and prevents obesity induced by high fat feeding or leptin deficiency

Kathy Jaworski^{1,2}, Maryam Ahmadian^{1,2}, Robin E. Duncan^{1,2}, Eszter Sarkadi-Nagy², Krista A. Varady², Marc K. Hellerstein², Hui-Young Lee³, Varman T. Samuel³, Gerald I. Shulman³, Kee-Hong Kim², Sarah de Val², Chulho Kang⁴, and Hei Sook Sul^{2,5}

²Department of Nutritional Science and Toxicology, University of California, Berkeley, CA 94720 USA

³Department of Internal Medicine, Yale University School of Medicine, New Haven, CT 06510 USA

⁴Department of Molecular and Cell Biology, University of California, Berkeley, CA 94720 USA

Abstract

A main function of white adipose tissue is to release fatty acids from triacylglycerol for other tissues to use as an energy source. While endocrine regulation of lipolysis has been extensively studied, autocrine/paracrine regulation is not well understood. Here, we describe the role of AdPLA, the newly identified major adipocyte phospholipase A₂, in the regulation of lipolysis and adiposity. AdPLA null mice have a markedly higher rate of lipolysis, due to increased cAMP levels arising from the marked reduction in adipose PGE₂ that binds the G α i-coupled receptor, EP3. AdPLA null mice have drastically reduced adipose tissue mass and triglyceride content, with normal adipogenesis. They also have higher energy expenditure with higher fatty acid oxidation within adipocytes. AdPLA deficient *ob/ob* mice remain hyperphagic but lean, with increased energy expenditure, yet have ectopic triglyceride storage and insulin resistance. AdPLA is a major regulator of adipocyte lipolysis and critical for the development of obesity.

INTRODUCTION

Triacylglycerol (TAG) in adipose tissue is the major energy storage form in mammals. An imbalance between energy intake and expenditure can result in excess TAG accumulation in adipose tissue, resulting in obesity 1. In morbid obesity, although controversial, increased adipocyte number (hyperplasia) may occur through adipocyte differentiation of precursor cells present in adipose tissue 2. However, obesity is largely attributed to adipocyte hypertrophy that occurs when TAG synthesis exceeds breakdown (lipolysis), resulting in elevated TAG storage 1,3. Unlike TAG synthesis 4,5 that occurs at high levels in other tissues, including liver for VLDL production, lipolysis for the provision of fatty acids as an

Users may view, print, copy, and download text and data-mine the content in such documents, for the purposes of academic research, subject always to the full Conditions of use:http://www.nature.com/authors/editorial_policies/license.html#terms

⁵Corresponding Author: Hei Sook Sul, Department of Nutritional Science and Toxicology, 219 Morgan Hall, University of California, Berkeley, CA, 94720 USA. Telephone: 510-642-3978. Fax: 510-642-0535. hsul@nature.berkeley.edu.

¹These authors contributed equally

energy source for use by other tissues is unique to adipocytes 6. Lipolysis in adipocytes is tightly regulated by hormones that are secreted according to nutritional status. During fasting, lipolysis is stimulated by catecholamines that increase cAMP levels, whereas, in the fed state, lipolysis is inhibited by insulin 1,3. While regulation of lipolysis by these endocrine factors has been extensively studied, the local regulation of lipolysis in adipose tissue by autocrine/paracrine factors is not well understood.

We recently identified an adipocyte phospholipase A₂ (PLA₂) by microarray analysis that we named Adipose-specific phospholipase A₂ (AdPLA) 7 (also called PLA2G16, HRASLS3, HREV107, HREV107-3, MGC118754, H-REV107-1). AdPLA belongs to a new group of intracellular calcium-dependent PLA₂s. The PLA₂ superfamily of enzymes catalyze hydrolysis of the *sn*-2 ester bond of phospholipids 8. PLA₂s function in remodeling of membrane phospholipids by acylation/deacylation cycles 8. More importantly, since the *sn*-2 position of phospholipids is typically enriched in arachidonic acid and other unsaturated fatty acids, PLA₂s catalyze the initial rate-limiting step in the production of eicosanoids 9. Eicosanoids, including prostaglandins (PGs), are potent local mediators of signal transduction and are known to modulate many physiological systems and exert autocrine/paracrine action through binding to specific G-coupled receptors 10. Although their physiological significance is unclear, there are some reports that suggest PGs may modulate adipocyte differentiation *in vitro* 11–14. In mature adipocytes, depending on the concentrations used, some PGs have been reported to stimulate, inhibit or exert no effect on lipolysis 15,16. Regardless, since AdPLA is highly expressed only in adipose tissue, we hypothesized that it could play an important role in adipose-specific processes such as lipolysis through modulation of arachidonic acid provision for PG biosynthesis.

Here, we show that AdPLA is the major PLA₂ in adipose tissue, and regulates lipolysis in an autocrine/paracrine manner through PGE₂. We report that ablation of *Adpla* prevents obesity from high fat feeding or leptin deficiency by regulating lipolysis through the PGE₂/EP3/cAMP pathway.

RESULTS

***Adpla* is expressed at a high level primarily in adipose tissue**

As we have shown previously 7, the 1.3 kb *Adpla* mRNA and the 18 kDa AdPLA protein are expressed in mice at a high level only in white adipose tissue (WAT) and brown adipose tissue depots (BAT) (Fig. 1a). *Adpla* is found exclusively in adipocytes and not in the stromal vascular fraction of adipose tissue that contains preadipocytes (Fig. 1a). In humans, similar to mice, *Adpla* was undetectable by RT-PCR in skeletal muscle and barely detectable in liver, but was abundantly expressed in WAT (Fig. 1a). We measured expression of all currently known intracellular PLA₂s. 7 We detected *Adpla* at approximately 10³- to 10⁵-fold higher levels (Fig. 1b), indicating that AdPLA is the major PLA₂ in adipose tissue. We investigated *Adpla* regulation in different nutritional and hormonal states. *Adpla* mRNA level in epididymal WAT was low in fasted mice but rose drastically (by 8-fold) after feeding a high carbohydrate, fat-free diet ($P < 0.01$) (Fig. 1c). *Adpla* mRNA was also low in adipose tissue of streptozotocin-diabetic mice, but similarly increased by approximately 10-fold after insulin administration. We observed substantially higher *Adpla* mRNA in WAT of

genetically obese *ob/ob* mice that are hyperinsulinemic and have markedly higher adipose tissue TAG storage (Fig. 1c), and higher AdPLA protein levels in obese *ob/ob* and *db/db* mice than in lean WT mice in both the fasted and refeed states (Fig. 1c). *Adpla* is therefore highly and specifically expressed in adipocytes and is upregulated by feeding/insulin and in obesity.

***Adpla* null mice have reduced adiposity and are resistant to diet-induced obesity**

To elucidate the physiological role of AdPLA, we used gene targeting to generate *Adpla* null mice (Suppl. Fig. 1) that we compared with wild-type littermates under a mixed genetic background (C57BL/6J and 129 SVJ) as well as on a C57BL/6J background (genetic backgrounds of mice utilized in specific experiments are indicated in the Methods). Although total body weights did not differ at weaning, at 11 wks, *Adpla* null mice fed a high fat diet (HFD) began to gain weight at a slower rate than wild-type littermates (Fig. 1d). This disparity in body weight was exacerbated as mice aged such that by 64 wks of age, *Adpla* null mice fed a HFD weighed only 39.1 ± 0.2 g ($n = 3$), versus wild-type littermates that weighed 73.7 ± 0.3 g ($n = 3$), $P < 0.001$. The decreased weight gain was also observed in *Adpla* null mice fed a standard chow diet (SD), albeit to a lesser extent (Fig. 1d). Food intakes in *Adpla* null and wild-type mice were equivalent, despite differences in body weights (0.09 g d^{-1} g BW^{-1} , $n = 6$).

The lower body weight of *Adpla* null mice was largely accounted for by a reduction in WAT weight. Body composition analysis indicated that *Adpla* null mice had decreased TAG content (Suppl. Table 1). At 18 wks, *Adpla* null mice fed a HFD had substantially smaller WAT depots compared to wild-type littermates with a combined WAT depot weight that was 74% lower (Fig. 2a). This difference increased further as the mice aged. We observed the same pattern of lower body and fat pad weight in *Adpla* null mice fed a SD, and in *Adpla* null mice under a C57BL/6J background (data not shown).

By standard pathology analysis, *Adpla* null mice showed no evidence of any gross, microscopic, or functional abnormalities, aside from reduced adiposity. However, as described in later sections, upon HFD feeding we detected enlarged livers in *Adpla* null mice with increased liver TAG content (Supplementary Table 1), although liver function was largely normal (Supplementary Fig. 2). Moreover, blood cell profile and immunological parameters in serum and adipose tissue were not changed in these mice compared to wild-type (Supplementary Fig. 2), and the weights of other organs were similar between the two groups (data not shown).

***Adpla* null mice have smaller adipocytes rather than impaired adipocyte differentiation**

A decrease in adipose tissue mass can result from a reduction in adipocyte size and/or a reduction in adipocyte number due to impaired differentiation. Evidence indicates that AdPLA deficiency did not significantly affect adipocyte differentiation. Expression levels of adipogenic transcription factors 17,18 including CCAAT/enhancer binding protein alpha (*C/ebpa*) and peroxisome proliferator-activated receptor gamma (*Pparg*) as well as the preadipocyte marker preadipocyte factor 1 (*Pref1*), were similar in wild-type and *Adpla* deficient WAT, as were late markers of adipocyte differentiation, including fatty acid

synthase (*Fas*), diglyceride acyltransferase 1 (*Dgat1*), and adipocyte fatty acid binding protein (*aP2/aFabp*) (Fig. 2b). DNA content in the fat depots of *Adpla* null and wild-type mice also did not differ significantly ($140.4 \pm 22.6 \mu\text{g}$ versus $123.7 \pm 14.6 \mu\text{g}$ DNA per fat pad, respectively, $n = 6$). We employed mouse embryonic fibroblasts (MEF) from wild-type and *Adpla* null embryos as well as 3T3-L1 cells transfected with *Adpla* or control vector. After undergoing differentiation to adipocytes in high insulin containing media, there were no differences between wild-type and *Adpla* null MEF or between *Adpla* overexpressing and control 3T3-L1 cells with regards to rounded adipocyte morphology or Oil red O staining (Fig. 2b). Expression of adipocyte markers such as *C/ebpa*, *Pparg*, *aP2/aFabp* and *Pref1* were also similar between wild-type and *Adpla* null MEF, confirming the same degree of differentiation (Fig. 2b).

Histological analysis showed that epididymal WAT from *Adpla* null mice contained a significantly greater frequency ($P < 0.05$) of the smallest adipocytes and a lower frequency of the mid-sized and largest adipocytes ($P < 0.01$) (Fig. 2c). We also found drastically decreased TAG content in adipose tissue of *Adpla* null mice (Fig. 2a). *Adpla* ablation therefore causes adipocyte hypotrophy due to lower TAG accumulation and smaller adipocyte size, rather than impaired adipocyte differentiation.

***Adpla* ablation increases lipolysis in adipose tissue**

To investigate if the drastically decreased adiposity observed in AdPLA null mice was due to increased lipolysis, we measured *in vivo* TAG metabolism over a two week period using a recently developed heavy water labeling technique 19. The fractional contribution of TAG-glycerol synthesis to adipose tissue TAG was significantly higher in *Adpla* null mice, reflecting a greater than 2-fold higher rate of replacement of preexisting TAG molecules with newly labeled TAG-glycerol, indicating increased TAG turnover (Fig. 3a). In agreement, the net *in vivo* lipolytic rate, calculated from the absolute rate of new TAG synthesis and the change in adipose tissue mass, was also 4- to 6-fold higher per gram of adipose tissue in *Adpla* null mice compared to wild-type mice (Fig. 3b). We measured [$U\text{-}^{14}\text{C}$]palmitate incorporation into TAG in adipose tissue explants and found similar incorporation in wildtype or AdPLA null mice, indicating comparable WAT fatty acid esterification in these animals (Fig. 3C). Therefore, we conclude that TAG hydrolysis, but not synthesis, is altered in WAT of AdPLA null mice.

To further investigate the effect of *Adpla* ablation on lipolysis, we compared basal and stimulated glycerol and fatty acid release from explants of WAT from *Adpla* null and wild-type mice (Fig. 3d). Under basal conditions, rates of glycerol and fatty acid release were significantly higher in adipose tissue from *Adpla* null mice. Furthermore, isoproterenol-stimulated lipolysis was also higher in *Adpla* deficient adipose tissue. Notably, the molar ratio of FFA to glycerol released from WAT explants was lower in AdPLA null mice (Fig. 3e). Because of the heterogeneity of cell populations within WAT explants, we also examined the effect of *Adpla* ablation on lipolysis in adipocytes differentiated from MEF that were isolated from *Adpla* null embryos. Probably due to the very high level of insulin in the media, the basal rate of lipolysis was very low in these cells and we could not detect differences in basal lipolysis between adipocytes differentiated from wild-type and *Adpla*

null MEF (Fig. 3f). This finding is in agreement with the comparable lipid content in MEF differentiated adipocytes (Fig. 2b). However, isoproterenol stimulated lipolysis, measured as free fatty acid release, was significantly higher in adipocytes differentiated from *Adpla* null MEF (Fig. 3f). These results clearly indicate that lack of *Adpla* results in increased lipolysis in adipose tissue.

***Adpla* null mice have reduced total PLA activity and PGE₂ levels in adipose tissue**

PLA activity in WAT was dramatically reduced by 82% in *Adpla* null mice (from 3.71 pmol mg⁻¹ min⁻¹ in wild-type to only 0.66 pmol mg⁻¹ min⁻¹) (Fig. 4a), while expression of other PLA₂s was unchanged. This finding establishes AdPLA as the major PLA in adipose tissue. Given the inverse relationship between PLA activity and lipolysis in *Adpla* null mice, we hypothesized that AdPLA may function in adipose tissue to regulate lipolysis locally by generating arachidonic acid for the production of PGs. We first measured levels in wild-type mice of PGs known to be found in adipose tissue. PGE₂ was present at significantly higher levels than any other PGs which were detected at levels well below effective concentrations required for binding to their cognate receptors 20 (Fig. 4b). We next determined expression levels in adipose tissue of the receptors for these PGs and found that EP3 was detected at a markedly higher level than other receptors examined including IP, DP, and EP1 (all undetectable) as well as EP2 and EP4 that were present at much lower levels (Fig. 4b). When we compared the levels of various PGs in adipose tissue from *Adpla* null and wild-type mice (Fig. 4b), we found that PGF₂α and 15-deoxy- 12,14-PGJ₂ that have been reported to affect adipocyte differentiation *in vitro* 13,21,22 were unchanged in *Adpla* deficient adipose tissue. However, PGE₂ levels were reduced to 12% of wild-type levels in *Adpla* deficient adipose tissue. PGI₂ levels were also significantly reduced. However, PGI₂ concentrations were well below those required for receptor activation, and IP was not detected in adipose tissue. Since PGE₂ and EP3 were found in adipose tissue at the highest levels, and since PGE₂ level was the most drastically affected of the PGs in *Adpla* null adipose tissue, we postulated that the change in PGE₂ through EP3 may have been a major contributor to the observed effects.

If AdPLA regulates the production and release of PGE₂ that can bind Gαi-coupled EP3, then cAMP levels should be increased in adipose tissue of *Adpla* null mice. Indeed, we detected an approximate 2-fold increase in cAMP levels relative to wild-type (Fig. 4c) and found significantly higher phosphorylation of hormone-sensitive lipase (HSL) in the absence of a change in HSL or desnutrin/ATGL protein levels (Fig. 4d). Our results support the idea that AdPLA that is induced by feeding/insulin, inhibits lipolysis by increasing PGE₂ that, in turn, activates EP3 and thereby decreases cAMP levels. In this regard, addition of exogenous PGE₂ decreased lipolysis to wild-type levels in differentiated adipocytes derived from *Adpla* null MEF (Fig. 4e) and in WAT explants (data not shown) as well as in isolated adipocytes from *Adpla* null mice (Fig. 4f). The addition of PGE₂ also restored cAMP levels in adipocytes isolated from *Adpla* null mice (Fig. 4g). Addition of L826266, an EP3 antagonist, prevented the anti-lipolytic effect of PGE₂ in adipocytes (Fig. 4h), providing evidence that EP3 mediates the anti-lipolytic effect of PGE₂.

***Adpla* ablation prevents obesity in *ob/ob* mice**

To test whether *Adpla* deficiency could prevent genetic obesity such as that caused by leptin deficiency, we introduced *Adpla* deficiency into *ob/ob* mice to generate double knockout (dKO) mice. On a SD, dKO mice gained drastically less weight than *ob/ob* mice (Fig. 5a,b). Striking differences in body weights were apparent by as early as 6 wks and became even more pronounced with age. Surprisingly, differences were not attributable to a reduction in food consumption since intakes were, in fact, somewhat increased in dKO mice compared to *ob/ob* mice (Fig. 5b). However, dKO mice exhibited reduced adiposity with a marked reduction in the weight of WAT depots compared to *ob/ob* mice (Fig. 5c). Other organ weights, except for the increased liver weight, were similar between the two groups of mice (data not shown). Carcass analysis showed that body and carcass weights of *Adpla* null and dKO at 40 weeks of age were less than those of either wild-type or *ob/ob* mice, while the proportion of water and lean tissue mass was increased (Fig. 5d). Percent lipid was reduced by 81% in AdPLA null and 69% in dKO mice compared to wild-type and *ob/ob* mice, respectively reflecting the drastically leaner phenotype in AdPLA deficiency.

We observed significantly higher lipolysis in dKO mice under both basal and stimulated conditions compared to *ob/ob* mice (Fig. 5e) that was accompanied by an 86% reduction in PGE₂ levels (Fig. 5f) and a 4-fold increase in cAMP levels (Fig. 5g). In *ob/ob* mice, reflecting higher *Adpla* expression, PGE₂ levels were 2.6-fold higher compared to wild-type mice. Notably, PGE₂ levels in dKO mice did not differ from *Adpla* null mice, indicating that AdPLA dominantly regulates PGE₂ levels in adipose tissue. Taken together, these results indicate that *Adpla* deficiency drastically influences PGE₂ and cAMP levels to modulate lipolysis and adiposity, even in a genetic obesity caused by leptin deficiency.

***Adpla* ablation causes insulin resistance and ectopic fat storage**

Changes in adiposity are often associated with alterations in glucose and insulin homeostasis. *Adpla* null mice fed a SD showed an attenuated response to insulin during the insulin tolerance test (ITT), but glucose tolerance similar to wild-type mice (Supplementary Fig. 5), likely due to elevated insulin secretion (Supplementary Table 2). *Adpla* null mice fed a HFD had significantly impaired glucose clearance during glucose tolerance test (GTT) and an impaired response to insulin during ITT compared to wild-type littermates (Fig. 6a). In addition, we found that *Adpla* ablation further impaired glycemic control in *ob/ob* mice on both a SD (data not shown) and HFD, making dKO mice even more glucose and insulin intolerant than the already impaired *ob/ob* mice (Fig. 6b). In agreement with our findings from GTT and ITT, *Adpla* null mice fed a SD showed normal fasting glucose but elevated serum insulin, whereas HFD-fed mice had elevated fasting serum glucose and insulin compared to wild-type mice (Supplementary Table 2). Serum glucose and insulin levels were also elevated in dKO compared with *ob/ob* mice on either diet (Supplementary Table 2).

To discern the impact of *Adpla* ablation on peripheral and hepatic insulin action, we performed a hyperinsulinemic-euglycemic clamp. The glucose infusion rate necessary to maintain euglycemia in *Adpla* null mice was 77% lower than in wild-type mice, indicating severely blunted insulin-stimulated glucose uptake and metabolism (Fig. 6c and

Supplementary Fig. 5). Compared with wild-type mice, *Adpla* null mice showed a 50% decrease in whole-body glucose uptake (Fig. 6d), and 44% and 65% decreases ($P < 0.05$) in glycolysis and glycogen synthesis, respectively, indicating decreased glucose metabolism. In addition, we found that suppression of hepatic glucose production (HGP) by insulin during the clamp was severely blunted in *Adpla* null mice (Fig. 6e), indicating hepatic insulin resistance. We found no difference in gastrocnemius 2-deoxyglucose (2-DG) uptake between wild-type and *Adpla* null mice (Fig. 6f). Notably, epididymal WAT 2-DG uptake per gram was higher, although the drastic decrease in adipose tissue mass resulted in a 72% reduction in *total* insulin stimulated glucose uptake by this tissue (Fig. 6g) that may explain lower net whole body glucose metabolism.

The livers of *Adpla* null mice were pale-tan in color and enlarged with numerous, lipid-laden vacuoles in hepatocytes (Supplementary Fig. 5). Liver DAG levels that have been associated with insulin resistance 23 were also significantly increased in *Adpla* null mice compared with wild-type mice ($3.05 \pm 0.46 \mu\text{g mg}^{-1}$ tissue versus $1.47 \pm 0.38 \mu\text{g mg}^{-1}$ tissue, respectively, $P < 0.05$). Lipid staining with Oil Red O also showed higher intramyocellular TAG content in skeletal muscle, although we found no difference in skeletal muscle DAG content (data not shown) or IRS-1 phosphorylation (Supplementary Fig. 5).

We found that circulating levels of leptin and adiponectin were decreased in *Adpla* null mice on both a SD and HFD (Supplementary Table 2). Relative expression levels of these adipokines in WAT from HFD-fed mice were also decreased (1.0 ± 0.30 versus 0.25 ± 0.07 , $P < 0.01$ for leptin, and 1.0 ± 0.26 versus 0.28 ± 0.05 , $P < 0.01$ for adiponectin, in wild-type and *Adpla* null mice, respectively). Circulating levels of adiponectin were lower in *ob/ob* mice compared to dKO mice (Supplementary Table 2). Adiponectin has been shown to increase fatty acid oxidation in skeletal muscle 24. We found decreased phosphorylation of AMPK at Thr 172 and reduced expression of acyl-CoA oxidase in skeletal muscle of *Adpla* null mice, as well as lower oxidation of [U- ^{14}C]-palmitate (Supplementary Fig. 5).

Despite increased lipolysis, serum non-esterified fatty acid (NEFA) levels were not higher but lower in *Adpla* null mice on both a SD and HFD (Supplementary Table 2). Serum triglycerides were also lower in *Adpla* null and dKO mice, despite pronounced steatosis and hepatic insulin resistance (Supplementary Table 1). We found increased TAG clearance in mice upon oral lipid load but no difference in serum TAG when lipoprotein lipase was first inhibited by WR1339 injection (Supplementary Fig. 4). Although its significance is unclear, lipoprotein lipase expression was 2-fold higher in livers from *Adpla* null mice (Supplementary Fig. 4). Taken together, fatty acid uptake by the liver appears to be higher in *AdPLA* null mice.

***Adpla* null mice have increased energy expenditure and fatty acid oxidation in adipose tissue**

Total oxygen consumption was higher in *Adpla* null and dKO mice compared with wild-type and *ob/ob* mice, respectively (Fig. 6h), and these differences were not attributed to changes in ambulatory activity (data not shown). We first examined BAT, but found no significant difference in the morphology or weight of interscapular BAT, nor any change in mRNA levels of genes involved in thermogenesis in BAT when mice were housed at 4°C (data not

shown). In WAT from *Adpla* null mice, however, we detected a 5.5-fold upregulation of uncoupling protein 1 (*Ucp-1*), as well as upregulation of other genes involved in oxidative metabolism including 3.2- and 5-fold increases in expression of peroxisome proliferator-activated receptor delta (*Ppar- δ*), and deiodinase 2 (*Dio2*), respectively (Fig. 6i). We determined the production of $^{14}\text{CO}_2$ from [$\text{U-}^{14}\text{C}$] palmitate and found that fatty acid oxidation was increased by 37% in isolated adipocytes from *Adpla* null mice compared to wild-type mice (Fig. 6j). Fatty acid oxidation was significantly lower in adipocytes from *ob/ob* mice than wild-type mice, but was restored to wild-type levels in dKO mice. As shown in Fig. 3E, we observed a decrease in the molar ratio of FFA to glycerol released from WAT explant studies of *Adpla* null mice compared to wild-type mice. This change in molar ratio of fatty acid to glycerol in *Adpla* null mice indicates increased utilization of FFA within adipocytes and supports our finding of increased fatty acid oxidation in adipose tissue. These findings help to explain not only increased energy expenditure but also decreased NEFA in the circulation, despite higher lipolysis in *Adpla* null mice.

DISCUSSION

Adpla is highly expressed only in adipose tissue, where lipolysis is a major function. We postulated that, since PLA₂s catalyze the initial rate-limiting step in PG synthesis, AdPLA may regulate lipolysis locally by controlling the provision of arachidonic acid for the production of PGs. Since *Adpla* is induced by feeding/insulin, as well as in *ob/ob* and *db/db* models of obesity, we predicted that AdPLA likely plays an inhibitory role in lipolysis. Indeed, we found that AdPLA plays a major role in modulating adipose tissue lipolysis by regulating PGE₂ levels. As a result, ablation of *Adpla* in mice prevented obesity induced by feeding a HFD, or by leptin deficiency.

While the regulation of lipolysis by catecholamines and insulin has been extensively studied, the local regulation of lipolysis in adipose tissue by autocrine/paracrine factors remains unclear. We found that *Adpla* is expressed in adipocytes at a much higher level than any other known PLA₂s, and total PLA activity was greatly reduced in adipose tissue of *Adpla* null mice while expression of other known PLA₂s remained unchanged, revealing that AdPLA is the major PLA₂ in this tissue and may provide arachidonic acid for PG synthesis. Among the PGs that have previously been detected in adipose tissue, we found that PGE₂ is present at levels one to two orders of magnitude higher. Furthermore, PGE₂ levels are drastically decreased in *Adpla* null and dKO mice, providing evidence for a significant role for AdPLA in regulating PGE₂ synthesis. We found that the G α i coupled receptor, EP3, was predominant in adipose tissue, and a specific inhibitor of EP3 prevented the anti-lipolytic effect of PGE₂. These findings suggest that PGE₂ suppresses lipolysis by decreasing cAMP levels through EP3 activation during feeding/insulin when *Adpla* is drastically induced. Indeed, we found that cAMP levels were elevated in WAT of *Adpla* null and dKO mice, and PGE₂ treatment restored cAMP levels in *Adpla* null adipocytes to wild-type levels. In *Adpla* null WAT, HSL phosphorylation was increased, while total levels of HSL and desnutrin/ATGL were unchanged, suggesting that phosphorylation of HSL is likely an important mediator of increased lipolysis in these mice.

In vivo, lipolysis was markedly higher per gram of adipose tissue in *Adpla* null mice compared to wild-type mice. Furthermore, both basal and isoproterenol-stimulated lipolysis were increased in explants of *Adpla* deficient adipose tissue and in adipocytes isolated from *Adpla* null mice, and stimulated lipolysis was higher in adipocytes differentiated from *Adpla* null MEF. Exogenous PGE₂ rescued lipolytic rates in *Adpla* deficient adipocytes in all three model systems, showing AdPLA regulation of lipolysis in adipocytes via PGE₂ production. The cyclooxygenase inhibitors NS-398 26 and indomethacin 27 have been shown to enhance basal and stimulated lipolysis, respectively, in adipose tissue, consistent with our present findings that AdPLA plays an important role in regulating lipolysis through production of PGE₂. Furthermore, we demonstrate that an EP3 inhibitor prevents the anti-lipolytic effects of PGE₂, consistent with our proposed model of lipolysis regulation by AdPLA through PGE₂ signaling. Due to increased phosphorylation of HSL and unsuppressed lipolysis, *Adpla* null mice have drastically decreased TAG content in adipose tissue. This indicates that suppression of lipolysis by the local PGE₂ produced by adipocytes plays a critical role in regulating adipocyte lipolysis and demonstrates a role for the AdPLA/PGE₂/EP3/cAMP signaling pathway in development of excess adipose tissue mass/TAG storage and obesity. In support of this, PGE₂ levels were found to be higher in adipose tissue of obese human patients 28. Overall, the present study shows that AdPLA plays a critical regulatory role in the adipocyte dominant function of lipolysis through PGE₂ in an autocrine/paracrine manner.

Fatty acids such as arachidonic acid that are released by the action of PLA₂s have been shown to either stimulate or inhibit adipocyte differentiation 29–31. Similarly, selective cyclooxygenase-2 inhibitors 12,14, or prostaglandins themselves 11,13,21,22 were reported to induce or inhibit adipogenesis. PGF_{2α} via its FP receptor and 15-deoxy- 12,14-PGJ₂ as a PPAR_γ ligand, have been reported to affect *in vitro* adipocyte differentiation 13,21. PGD₂ may generate 15-deoxy- 12,14-PGJ₂ and PGI₂, and through its IP receptor, may also affect adipocyte differentiation *in vitro* 11,22. However, unlike PGE₂, we have found that these PGs are not detected at high enough concentrations in adipose tissue to effectively bind their receptors 20, which were also barely detectable in adipose tissue. PGs other than PGE₂, therefore, may not play a significant role. In our study, PGE₂ was the most abundant PG found in adipose tissue. However, our results clearly show that adipocyte differentiation, either *in vitro* or *in vivo*, was not affected by AdPLA.

The increased cAMP levels in WAT resulted in increased lipolysis and, consequently, decreased adipocyte size with lower TAG content in *Adpla* null and dKO mice, despite similar food intakes. TAG content in *Adpla* null mice and dKO mice was markedly lower than wild-type and *ob/ob* mice, respectively. Although increased lipolysis in *Adpla* null mice resulted in ectopic TAG accumulation in the liver and skeletal muscle, this could not fully account for the loss of TAG from adipose tissue. Indeed, oxygen consumption was increased in *Adpla* null and dKO mice. While we did not detect any changes in BAT, surprisingly, *Ucp-1*, *Dio2* and *Ppard* in WAT of *Adpla* null mice were significantly increased, suggesting higher oxidation and thermogenesis in WAT. Ectopic expression of *Ucp-1* in WAT has been reported to cause resistance to diet-induced obesity with increased fatty acid oxidation in adipocytes 32. Consistent with this, we found significantly increased fatty acid oxidation in

adipocytes from *Adpla* null and dKO mice compared with wild type and *ob/ob* mice, respectively, indicating that, at least in part, increased fatty acid utilization within adipocytes contributed to the increased energy expenditure.

Adpla null and dKO mice are extremely lean but insulin resistant. Results from hyperinsulinemic-euglycemic clamping studies indicate that insulin resistance in *Adpla* null mice is due to hepatic insulin resistance as well as reduced peripheral glucose metabolism. Interestingly, there was no difference in insulin-stimulated skeletal muscle glucose uptake between wild-type and *Adpla* null mice, but total insulin stimulated glucose-uptake was lower in WAT due to the drastic reduction in the mass of this tissue. It is interesting to note that despite severe insulin resistance and increased lipolysis in *Adpla* null mice, serum NEFA levels were lower in these mice. The molar ratio of FFA to glycerol release from adipose tissue was significantly lower in *Adpla* null mice, suggesting increased utilization of fatty acids within adipose tissue. Consistent with this finding, we observed increased fatty acid oxidation in adipose tissue. Ectopic storage of TAG in liver and skeletal muscle suggests that removal of FFA from the circulation by these tissues may potentially have been increased and therefore may also have contributed to decreased serum NEFA levels. However, it is most likely that even with the higher rate of lipolysis, the drastically reduced adipose tissue mass in *Adpla* null mice resulted, overall, in lower net FFA liberation. Indeed, other mouse models with increased lipolysis and decreased adipose tissue also reported unchanged or reduced serum NEFA 33–36.

Adpla expression in humans is also adipose-specific. Currently, little is known regarding the pathological phenotype of individuals lacking AdPLA. Database search for single nucleotide polymorphisms (SNPs) in the *Adpla* gene in humans identified one SNP (Ser48Ala) within the coding region. An additional 230 SNPs have also been detected within non-coding regions of the *Adpla* gene. It is not known whether these result in altered protein function or levels, and clinical associations for these have not been reported, most likely because the present study is the first to characterize the physiological role of AdPLA. Many questions remain regarding the effect of partial or total *Adpla* gene ablation in humans, and further research in this area will yield advances in understanding the pathology of human obesity as well as type 2 diabetes.

METHODS

Cell culture

We isolated, maintained and differentiated MEF and 3T3-L1 as previously described 37.

RNA analysis

We subjected total RNA isolated with Trizol reagent (Invitrogen) to Northern blotting (Amersham) or to RT-qPCR or RT-PCR. Primers utilized with the ABI PRISM 7700 sequence fast detection system (PE Applied Biosystems) were pre-validated for efficiency of amplification that was reported to be the same for all and essentially 100%.

Western Blotting

We separated proteins by 12% SDS-PAGE, transferred to nitrocellulose and probed with primary antibodies against AdPLA, phospho-AMPK α (Thr172), AMPK α , HSL, desnutrin/Atgl, phosphoserine, IRS-1, phospho-IRS-1 (Ser307), Gapdh, or β -actin.

Lipolysis

We performed lipolysis studies in adipocytes isolated as previously described³⁸ from gonadal WAT, and in explants from freshly removed epididymal fat pads (~20 mg) and MEF differentiated to adipocytes. Samples were incubated in Krebs-Ringer medium buffered with bicarbonate plus HEPES with 3.5% fatty acid-free BSA and 0.1% glucose (KRB), with or without 200 nM isoproterenol (Sigma), PGE₂ (Cayman), adenosine deaminase (Calbiochem), 0.5 μ M Triacsin C (Biomol) or L826266 (Merck Frosst Canada), and measured glycerol (Sigma) and fatty acid (Wako). We determined prostaglandin levels by competitive enzyme immunoassay (R&D) after solid phase extraction by SPE cartridges (C-18) (Cayman), and cAMP levels by competitive immunoassay (R&D).

Mouse maintenance

All studies received approval from the University of California at Berkeley Animal Care and Use Committee. We utilized mice on a pure C57BL/6J background, after backcrossing for 10 generations, for studies of lipolysis, energy expenditure, hyperinsulinemic-euglycemic clamping, fatty acid oxidation, TAG clearance, and for all studies on dKO mice. In all other experiments, we compared *Adpla*^{-/-} and wild-type littermates in a mixed genetic background (C57BL/6J and 129 SVJ), but the results were also confirmed in a C57BL/6J background. We provided either a SD or a HFD (45 kcal% fat, 35 kcal% carbohydrate and 20 kcal% protein, Research Diets) *ad libitum*. To generate *ob/ob* mice deficient in *Adpla*, heterozygous C57BL/6J *ob*^{-/+} mice (Jackson Laboratory) were bred with *Adpla*^{-/-} mice under a C57BL/6J background resulting in heterozygotes that were interbred to produce dKO mice.

Carcass and tissue analysis

We homogenized frozen, eviscerated carcasses from 40 wk-old mice fed a HFD in water, dried the homogenates to a constant weight, and estimated lipid content by the method of Bligh and Dyer³⁹. We extracted tissue neutral lipids by the method of Folch⁴⁰, isolated TAG and DAG by TLC, and quantitated lipids using Infinity reagent (Thermo Trace) after sonification in 1% Triton X-100.

Glucose and insulin tolerance tests

For GTT, we injected mice intraperitoneally with D-glucose (WT or KO, 2 mg/g BW; dKO or *ob/ob* mice, 0.625 mg/g BW) following an overnight fast and monitored tail blood glucose levels. For ITT, mice were injected with insulin (humulin, Eli Lilly) at a level of 0.5 mU/g BW (WT and KO mice on a SD), 0.75 mU/g BW (WT and KO mice fed a HFD) or 1.75 mU/g BW (*ob/ob* and dKO) after a 5 h fast.

Hyperinsulenemic-euglycemic clamp

We implanted jugular venous catheters seven days prior to the study. After an overnight fast, we infused [$3\text{-}^3\text{H}$]glucose (Perkin Elmer) at a rate of $0.05\ \mu\text{Ci}\ \text{min}^{-1}$ for 2 hours to assess basal glucose turnover, followed by the hyperinsulinemic-euglycemic clamp for 140 min with a primed/continuous infusion of human insulin ($300\ \text{pmol}\ \text{kg}^{-1}$ prime ($43\ \text{mU}\ \text{kg}^{-1}$)) over 3 min, followed by $42\ \text{pmol}\ \text{kg}^{-1}\ \text{min}^{-1}$ ($6\ \text{mU}\ \text{kg}^{-1}\ \text{min}^{-1}$) infusion (Novo Nordisk, Princeton, NJ), a continuous infusion of [$3\text{-}^3\text{H}$]glucose ($0.1\ \mu\text{Ci}\ \text{min}^{-1}$), and a variable infusion of 20% dextrose to maintain euglycemia ($\sim 100\text{--}120\ \text{mg}\ \text{dl}^{-1}$). We obtained plasma samples from the tail and measured tissue-specific glucose uptake after injection of a bolus of $10\ \mu\text{Ci}$ of 2-deoxy-D-[$1\text{-}^{14}\text{C}$]glucose (Perkin Elmer) at 85 min⁴¹. We analyzed our results as previously described⁴².

Histological analysis

We embedded tissues in paraffin and stained $6\ \mu\text{m}$ thick sections with hematoxylin and eosin, and determined adipocyte cell size using image J software measuring at least 300 cells from each sample.

PLA activity

We assayed supernatants of WAT for PLA activity by monitoring the liberation of [^{14}C]palmitate from 1,2-di[$1\text{-}^{14}\text{C}$]palmitoyl-*sn*-glycero-3-phosphocholine as previously described⁴³.

Indirect calorimetry and body temperature

We measured oxygen consumption (VO_2) using the Oxymax system (Columbus Instruments).

$^2\text{H}_2\text{O}$ Labeling and GC-MS Analysis

We extracted lipids from gonadal fat pads of mice administered $^2\text{H}_2\text{O}$ in drinking water for a 2-week period, trans-esterified the lipid phase by incubation with 3 N methanolic HCl and separated glycerol from fatty acid (FA)-methyl esters using the Folch technique⁴⁰. We lyophilized and derivatized the aqueous phase containing free glycerol to glycerol triacetate by incubation with acetic anhydride-pyridine (2:1). We employed a model 6890 GC with 5973 mass spectrometer (Agilent Technologies), fitted with a DB-225 fused silica column (J&W). We analyzed glycerol-triacetate under chemical ionization conditions by selected ion monitoring of mass-to-charge ratios (m/z) 159–161 (representing $\text{M}_0\text{--}\text{M}_2$) and FA-methyl esters as described elsewhere¹⁹.

We measured fractional TAG-glycerol synthesis as described^{19,44}:

$$f_{\text{TAG}} = \text{EM}_{1\text{-TAG-glycerol}} / A_{1\infty\text{-TAG-glycerol}}$$

We estimated net lipolysis from f_{TAG} synthesis and adipose mass as follows: [$f_{\text{TAG}} \times (\text{adipose mass} / \text{labeling time}) - (\text{adipose mass} / \text{labeling time})$] / fat pad mass. Values with net lipolysis equivalent to zero were excluded from analysis.

Fatty Acid Oxidation

We determined fatty acid oxidation in isolated adipocytes as previously described 45.

Statistical Analysis

We assessed the results by Student's *t* test to compare two groups or by one-way ANOVA with Dunnett's post-hoc test for multiple comparisons and expressed them as means \pm SEM. We analyzed adipocyte size distribution by Wilcoxon Signed Rank Test.

Reference Sequences

Adpla is located on chromosome 19 in the mouse genome. Reference sequence identifiers for mouse *Adpla* are: gene (NT_039687.7), protein (NP_644675), and mRNA (NM_139269).

Supplementary Material

Refer to Web version on PubMed Central for supplementary material.

ACKNOWLEDGMENTS

This work was supported in part by DK75682 from the US National Institutes of Health to H. S. S. and DK59635 to G. I. S. R. E. D. and K. A. V. are recipients of Postdoctoral Fellowships from the Natural Sciences and Engineering Research Council of Canada. R. E. D. is a recipient of a Postdoctoral Fellowship from the Canadian Institutes of Health Research. The authors would like to thank O. Barauskas for technical help, D. Frasson for fatty acid oxidation measurement, Y. Wang for performing WR1339 injections, J. Lu, J. Chen, R. Mantara and N. Nag, for assistance with animal maintenance, A. Birkenfeld and D. Frederick for assistance with clamping studies, C. Lange and J. Chithalen for assistance with graphics, and Merck Frosst Canada for the kind gift of L826266.

REFERENCES

1. Duncan RE, Ahmadian M, Jaworski K, Sarkadi-Nagy E, Sul HS. Regulation of lipolysis in adipocytes. *Annu Rev Nutr.* 2007; 27:79–101. [PubMed: 17313320]
2. Gregoire FM, Smas CM, Sul HS. Understanding adipocyte differentiation. *Physiol Rev.* 1998; 78:783–809. [PubMed: 9674695]
3. Jaworski K, Sarkadi-Nagy E, Duncan RE, Ahmadian M, Sul HS. Regulation of triglyceride metabolism. IV. Hormonal regulation of lipolysis in adipose tissue. *Am J Physiol Gastrointest Liver Physiol.* 2007; 293:G1–G4. [PubMed: 17218471]
4. Dircks L SH. Acyltransferases of de novo glycerophospholipid biosynthesis. *Prog Lipid Res.* 1999; 38:461–479. [PubMed: 10793891]
5. Yet SF LS, Hahm YT, Sul HS. Expression and identification of p90 as the murine mitochondrial glycerol-3-phosphate acyltransferase. *J Biochem.* 1993:9486–9491.
6. Vance DE, Vance JE. *Biochemistry of lipids, lipoproteins and membranes.* 2002
7. Duncan RE, Sarkadi-Nagy E, Jaworski K, Ahmadian M, Sul HS. Identification and Functional Characterization of Adipose-specific Phospholipase A2 (AdPLA). *J Biol Chem.* 2008; 283:25428–25436. [PubMed: 18614531]
8. Schaloske RH, Dennis EA. The phospholipase A(2) superfamily and its group numbering system. *Biochim Biophys Acta.* 2006
9. Yuan C, Rieke CJ, Rimon G, Wingerd BA, Smith WL. Partnering between monomers of cyclooxygenase-2 homodimers. *Proc Natl Acad Sci U S A.* 2006; 103:6142–6147. [PubMed: 16606823]
10. Richelsen B. Release and effects of prostaglandins in adipose tissue. *Prostaglandins Leukot Essent Fatty Acids.* 1992; 47:171–182. [PubMed: 1475271]

11. Aubert J, et al. Prostacyclin IP receptor up-regulates the early expression of C/EBPbeta and C/EBPdelta in preadipose cells. *Mol Cell Endocrinol.* 2000; 160:149–156. [PubMed: 10715548]
12. Fajas L, Miard S, Briggs MR, Auwerx J. Selective cyclo-oxygenase-2 inhibitors impair adipocyte differentiation through inhibition of the clonal expansion phase. *J Lipid Res.* 2003; 44:1652–1659. [PubMed: 12837847]
13. Forman BM, et al. 15-Deoxy-delta 12, 14-prostaglandin J2 is a ligand for the adipocyte determination factor PPAR gamma. *Cell.* 1995; 83:803–812. [PubMed: 8521497]
14. Yan H, Kermouni A, Abdel-Hafez M, Lau DC. Role of cyclooxygenases COX-1 and COX-2 in modulating adipogenesis in 3T3-L1 cells. *J Lipid Res.* 2003; 44:424–429. [PubMed: 12576525]
15. Cohen-Luria R RG. Prostaglandin E2 can bimodally inhibit and stimulate the epididymal adipocyte adenyl cyclase activity. *Cell signal.* 1992; 4:331–335. [PubMed: 1510880]
16. Kather H, Simon B. Biphasic effects of prostaglandin E2 on the human fat cell adenylate cyclase. *J Clin Invest.* 1979; 64:609–612. [PubMed: 457871]
17. Smas CM SH. Pref-1, a protein containing EGF-like repeats, inhibits adipocyte differentiation. *Cell.* 1993; 73:725–734. [PubMed: 8500166]
18. Latasa MJ GM, Moon YS, Kang C, Sul HS. Occupancy and function of the –150 SRE and –65 E-box in nutritional regulation of the fatty acid synthase gene in living animals. *Mol Cell Biol.* 2003; 23:5896–5907. [PubMed: 12897158]
19. Turner SM, et al. Measurement of TG synthesis and turnover in vivo by 2H2O incorporation into the glycerol moiety and application of MIDA. *Am J Physiol Endocrinol Metab.* 2003; 285:E790–E803. [PubMed: 12824084]
20. Bell-Parikh LC, et al. Biosynthesis of 15-deoxy-delta12,14-PGJ2 and the ligation of PPARgamma. *J Clin Invest.* 2003; 112:945–955. [PubMed: 12975479]
21. Reginato MJ, Krakow SL, Bailey ST, Lazar MA. Prostaglandins promote and block adipogenesis through opposing effects on peroxisome proliferator-activated receptor gamma. *J Biol Chem.* 1998; 273:1855–1858. [PubMed: 9442016]
22. Vassaux G, Gaillard D, Ailhaud G, Negrel R. Prostacyclin is a specific effector of adipose cell differentiation. Its dual role as a cAMP- and Ca(2+)-elevating agent. *J Biol Chem.* 1992; 267:11092–11097. [PubMed: 1317853]
23. Savage DB, Petersen KF, Shulman GI. Disordered lipid metabolism and the pathogenesis of insulin resistance. *Physiol Rev.* 2007; 87:507–520. [PubMed: 17429039]
24. Yoon M-J, et al. Adiponectin increases fatty acid oxidation in skeletal muscle cells by sequential activation of AMP-activated protein kinase, p38 mitogen-activated protein kinase, and peroxisome proliferator-activated receptor. *Diabetes.* 2006; 55:2562–2570. [PubMed: 16936205]
25. Johansson SM, Yang JN, Lindgren E, Fredholm BB. Eliminating the antilipolytic adenosine A1 receptor does not lead to compensatory changes in the antilipolytic actions of PGE2 and nicotinic acid. *Acta Physiol.* 2007; 190:87–96.
26. Fain JN, Leffler CW, Bahouth SW. Eicosanoids as endogenous regulators of leptin release and lipolysis by mouse adipose tissue in primary culture. *J Lipid Res.* 2000; 41:1689–1694. [PubMed: 11013312]
27. Girouard H, Savard R. The lack of bimodality in the effects of endogenous and exogenous prostaglandins on fat cell lipolysis in rats. *Prostaglandins Other Lipid Mediat.* 1998; 56:43–52. [PubMed: 9674020]
28. Fain JN, Madan AK, Hiler ML, Cheema P, Bahouth SW. Comparison of the release of adipokines by adipose tissue, adipose tissue matrix, and adipocytes from visceral and subcutaneous abdominal adipose tissues of obese humans. *Endocrinology.* 2004; 145:2273–2282. [PubMed: 14726444]
29. Gaillard D, Negrel R, Lagarde M, Ailhaud G. Requirement and role of arachidonic acid in the differentiation of pre-adipose cells. *Biochem J.* 1989; 257:389–397. [PubMed: 2539084]
30. Massiera F, et al. Arachidonic acid and prostacyclin signaling promote adipose tissue development: a human health concern? *J Lipid Res.* 2003; 44:271–279. [PubMed: 12576509]
31. Petersen RK, et al. Arachidonic acid-dependent inhibition of adipocyte differentiation requires PKA activity and is associated with sustained expression of cyclooxygenases. *J Lipid Res.* 2003; 44:2320–2330. [PubMed: 12923227]

32. Kopecky J, Hodny Z, Rossmeisl M, Syrový I, Kozak LP. Reduction of dietary obesity in aP2-Ucp transgenic mice: physiology and adipose tissue distribution. *Am J Physiol*. 1996; 270:E768–E775. [PubMed: 8967464]
33. Hertzel AV, et al. Lipid metabolism and adipokine levels in fatty acid-binding protein null and transgenic mice. *Am J Physiol Endocrinol Metab*. 2006; 290:E814–E823. [PubMed: 16303844]
34. Lucas S, Tavernier G, Tiraby C, Mairal A, Langin D. Expression of human hormone-sensitive lipase in white adipose tissue of transgenic mice increases lipase activity but does not enhance in vitro lipolysis. *J Lipid Res*. 2003; 44:154–163. [PubMed: 12518034]
35. Martínez-Botas J, et al. Absence of perilipin results in leanness and reverses obesity in *Lepr(db/db)* mice. *Nat Genet*. 2000; 26:474–479. [PubMed: 11101849]
36. Tansey JT, et al. Perilipin ablation results in a lean mouse with aberrant adipocyte lipolysis, enhanced leptin production, and resistance to diet-induced obesity. *Proc Natl Acad Sci U S A*. 2001; 98:6494–6499. [PubMed: 11371650]
37. Kim KH, Lee K, Moon YS, Sul HS. A cysteine-rich adipose tissue-specific secretory factor inhibits adipocyte differentiation. *J Biol Chem*. 2001; 276:11252–11256. [PubMed: 11278254]
38. Viswanadha S, Londos C. Optimized conditions for measuring lipolysis in murine primary adipocytes. *J Lipid Res*. 2006; 47:1859–1864. [PubMed: 16675855]
39. Bligh EG, Dyer WJ. A rapid method of total lipid extraction and purification. *Can J Biochem Physiol*. 1959; 37:911–917. [PubMed: 13671378]
40. Folch J, Lees M, Sloane Stanley GH. A simple method for the isolation and purification of total lipides from animal tissues. *J Biol Chem*. 1957; 226:497–509. [PubMed: 13428781]
41. Youn JH, Buchanan TA. Fasting does not impair insulin-stimulated glucose uptake but alters intracellular glucose metabolism in conscious rats. *Diabetes*. 1993; 42:757–763. [PubMed: 8482433]
42. Samuel VT, et al. Targeting *foxo1* in mice using antisense oligonucleotides improves hepatic and peripheral insulin action. *Diabetes*. 2006; 55:2042–2050. [PubMed: 16804074]
43. Lucas KK, Dennis EA. Distinguishing phospholipase A2 types in biological samples by employing group-specific assays in the presence of inhibitors. *Prostaglandins Other Lipid Mediat*. 2005; 77:235–248. [PubMed: 16099408]
44. Chen JL, et al. Physiologic and pharmacologic factors influencing glyceroneogenic contribution to triacylglyceride glycerol measured by mass isotopomer distribution analysis. *J Biol Chem*. 2005; 280:25396–25402. [PubMed: 15888453]
45. Bansode RR, Huang W, Roy SK, Mehta M, Mehta KD. Protein kinase C β deficiency increases fatty acid oxidation and reduces fat storage. *J Biol Chem*. 2008; 283:231–236. [PubMed: 17962198]

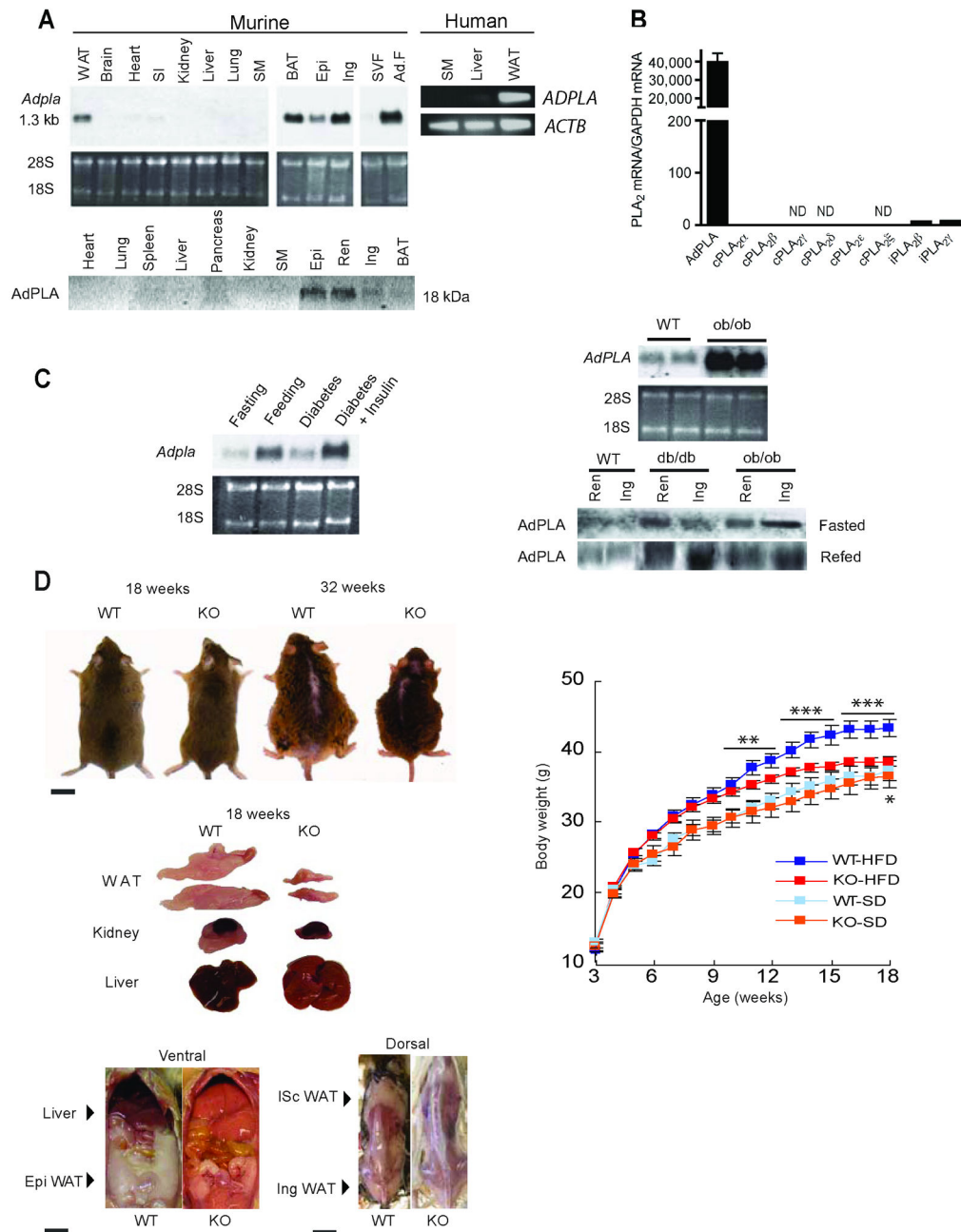


Figure 1. *Adpla* tissue distribution, regulation of expression, and body weights of *Adpla* null mice. (a) Top panel (left side): 10 μg of total RNA from various mouse tissues were analyzed by Northern blotting. SI (small intestine), SM (skeletal muscle), Epi (epididymal fat), Ing (inguinal fat), SVF (stromal vascular fraction), Ad.F (adipocyte fraction). Top panel (right side): RNA (2.5 μg) from human SM, liver, or WAT were analyzed by RT-PCR for expression of *Adpla* or β-actin. Bottom panel: Western blot analysis for AdPLA protein in various mouse tissues. 80 μg of protein was subjected to SDS-PAGE and probed with anti-

AdPLA antibodies. Ren (renal fat). **(b)** RT-qPCR using RNA from wild-type (WT) renal WAT. Values for PLA₂s were normalized to *Gapdh* and then expressed relative to *cPLA2-α* ($n = 5$). ND = not detected. **(c)** Left panel: Northern blot of *Adpla* mRNA in epididymal WAT from mice fasted for 48 h or fasted and refed for 12 h, or made diabetic by streptozotocin injection, with or without insulin replacement ($n = 3$). Right upper panel: *Adpla* mRNA expression in inguinal WAT from WT and *ob/ob* mice analyzed by Northern blotting ($n = 3$). Right lower panel: Western blotting for AdPLA in WAT depots from WT, *db/db* and *ob/ob* mice ($n = 3$). **(d)** Top left panel: Representative photographs of male WT and *Adpla* null (KO) mice at 18 and 32 wks of age. Scale bar = 15 mm. Top right panel: Body weights of male WT and KO on either a SD ($n = 11$), or a HFD ($n = 24-33$). Bottom left panels: Representative photographs of fat pads and organs of 18 wk-old male KO and WT littermates, ISc (interscapular). Scale bar left = 8 mm; Scale bar right = 10 mm. Results are means \pm SEM, ** $P < 0.01$, *** $P < 0.001$ versus WT.

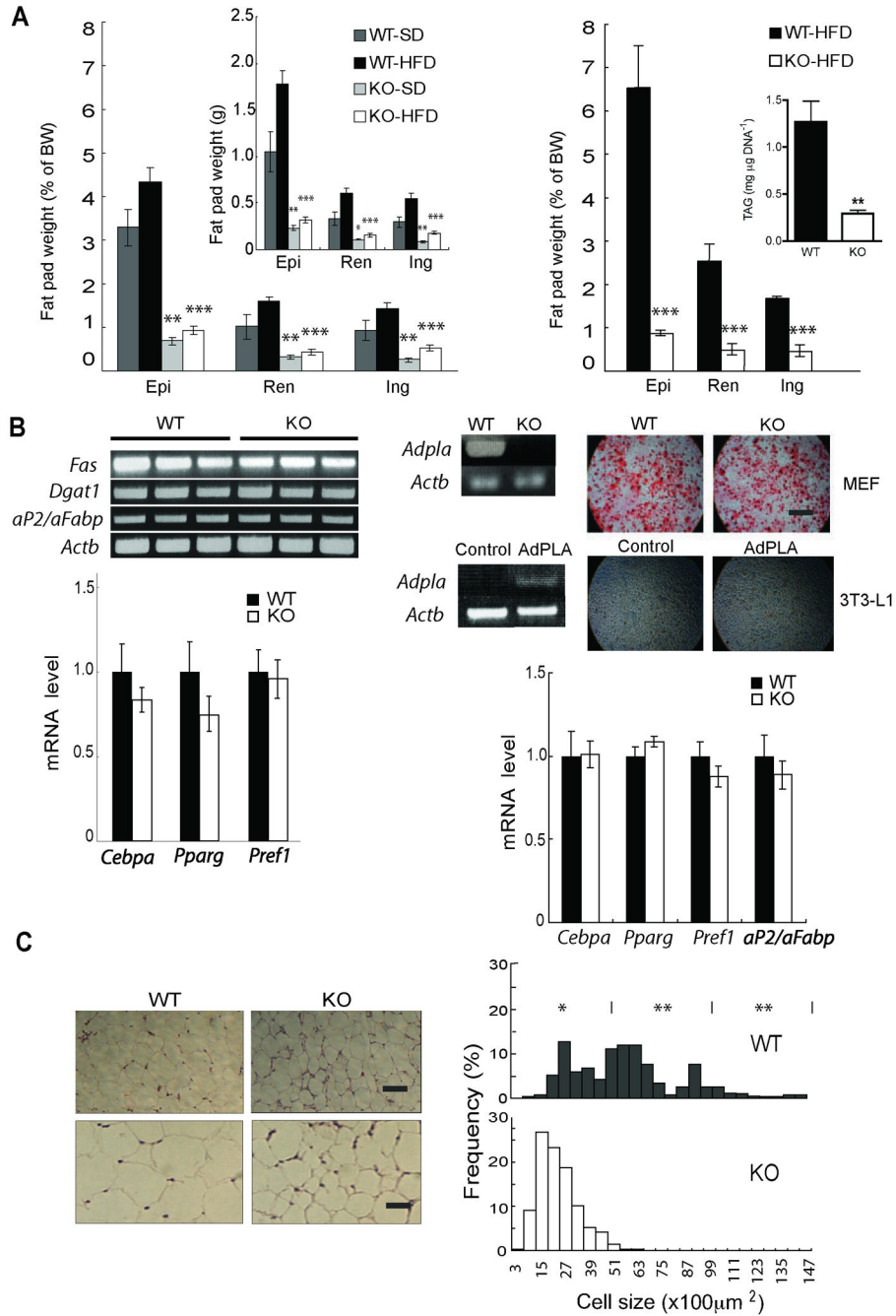
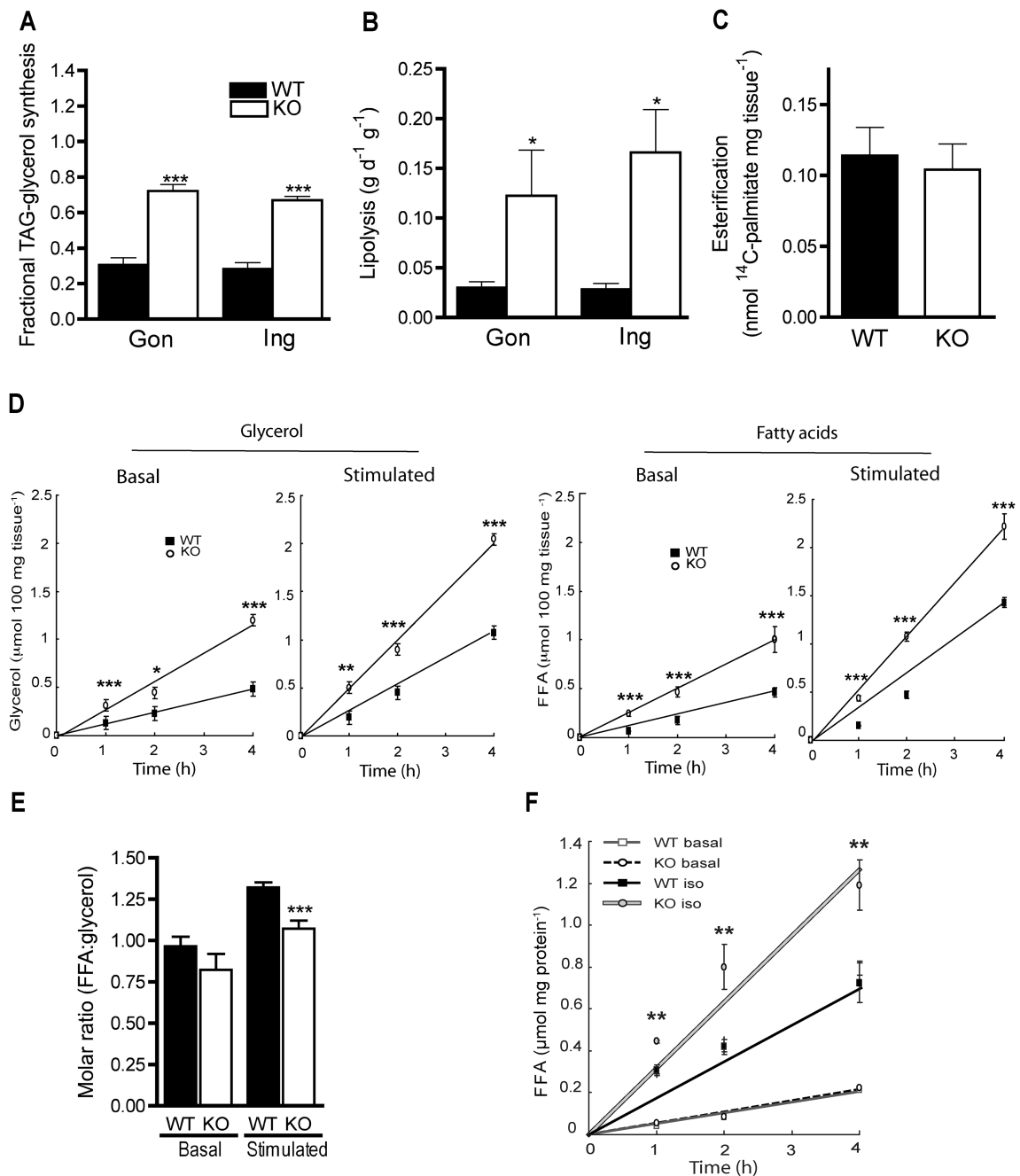


Figure 2. *Adpla* ablation causes a reduction in fat pad weight, TAG content, and adipocyte size, but does not affect adipocyte differentiation. (a) Left panel: Fat pad weights from male KO and WT littermates. Mice were fed a SD or a HFD until 18 wks of age ($n = 6-16$). Right panel: Fat pad weights of male KO and WT littermates on a HFD at 32 wks of age ($n = 8$). Inset: TAG content in epididymal WAT. (b) Left top panel: RT-PCR for genes involved in lipid metabolism, using RNA from epididymal WAT of male WT and KO ($n = 5$). Left bottom panel: RT-qPCR for adipocyte differentiation markers, using RNA from epididymal WAT

of 18 wk-old male mice ($n = 5$). Upper right panels: MEF from WT and KO embryos were differentiated and harvested at d 12, or stained with Oil Red O. 3T3-L1 cells transfected with LacZ control vector or *Adpla* expression vector were also differentiated and stained for neutral lipid. *Adpla* mRNA levels were determined in cells by RT-PCR using *Gapdh* as a control. Right bottom panel: RT-qPCR of adipogenic markers using RNA from adipocytes differentiated from WT and KO MEF ($n = 4$). Scale bar = 6 mm. (c) Left panel: Paraffin-embedded sections of epididymal WAT from 18 wk-old male KO and WT mice fed a HFD were stained with hematoxylin and eosin. Scale bar top = 80 μm ; Scale bar bottom = 20 μm . Right panel: Distribution of adipocyte size. Results are means \pm SEM, * $P < 0.05$, ** $P < 0.01$, *** $P < 0.001$ versus WT.

**Figure 3.**

Adpla ablation increases lipolysis *in vivo*, *ex vivo* and *in vitro*. (a) Fractional *in vivo* synthesis of TAG-glycerol in gonadal (Gon) and inguinal (Ing) WAT of 24 wk old female mice on a HFD ($n = 5-6$). (b) *In vivo* lipolysis in Gon and Ing WAT from 24 wk old female mice on a HFD ($n = 3-6$). (c) ^{14}C -palmitate esterification into TAG in WAT explants. (d) Basal and stimulated (+ 100 nM isoproterenol) lipolysis measured by glycerol (left panel) and fatty acids (right panel) released from explants of epididymal WAT from overnight fasted 16 wk old male WT and KO mice on a HFD ($n = 5$). (e) Molar ratio of FFA to

glycerol release from WAT explants. (f) Basal and stimulated lipolysis as measured by fatty acids released from WT and KO MEF at d 12 after differentiation into adipocytes. MEF were incubated with or without isoproterenol at 200 nM ($n = 6$). Results are means \pm SEM, $*P < 0.05$, $**P < 0.01$, $***P < 0.001$.

Author Manuscript

Author Manuscript

Author Manuscript

Author Manuscript

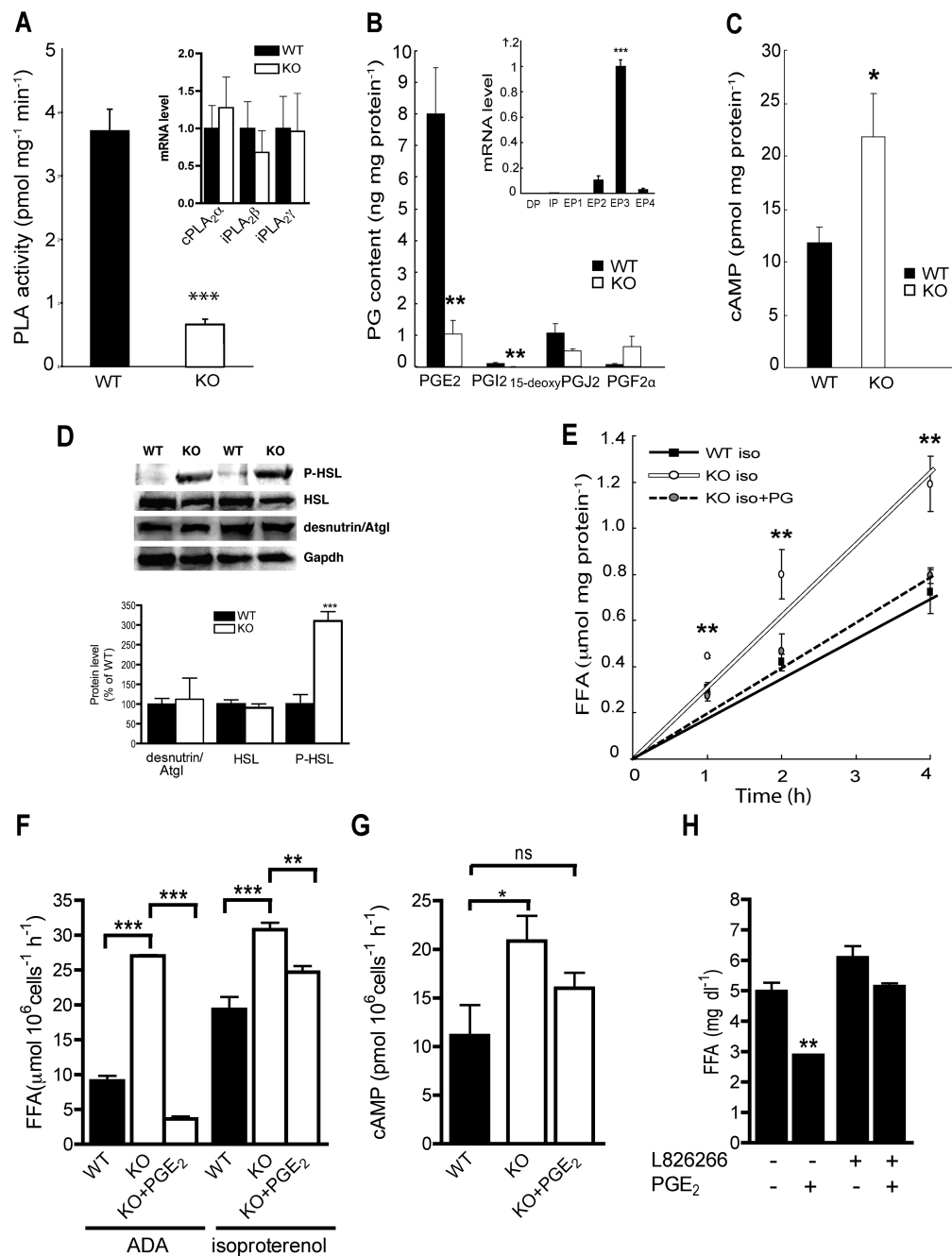
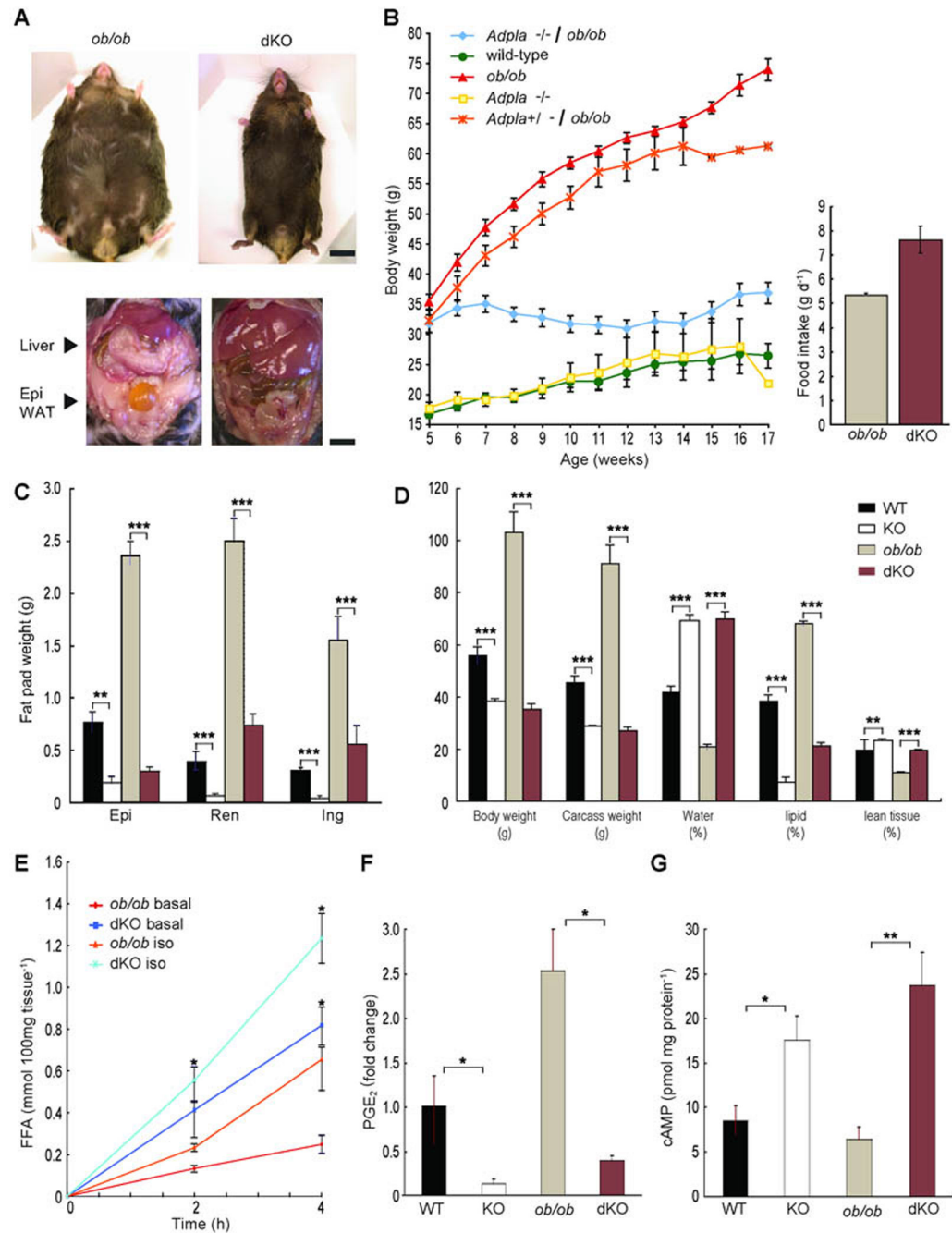


Figure 4. *Adpla* deficiency increases lipolysis by decreasing PGE₂ levels and increasing cAMP levels. (a) Total PLA activity in epididymal WAT from 16 wk old male WT and KO mice fed a HFD (*n* = 3). Inset: PLA₂ expression in WAT. (b) PG content in epididymal WAT of 18 wk old male WT and KO mice on a HFD (*n* = 5). Inset: RT-qPCR of PG receptors normalized to *Actb*, in WAT of WT mice (*n* = 5). (c) cAMP in epididymal WAT from male WT and KO mice on a HFD (*n* = 5). (d) Immunoblot of phosphorylated Hsl (P-Hsl), Hsl, desnutrin/Atgl and Gapdh (control) with relative quantification. (e) Stimulated lipolysis measured by fatty

acid release from WT and KO MEF on d 12 after differentiation into adipocytes. MEF were incubated with 200 nM isoproterenol and 100 nM PGE₂ as indicated ($n = 6$). (f) Lipolysis in isolated adipocytes from KO or WT mice incubated with 1 U ml⁻¹ adenosine deaminase (ADA) or isoproterenol (200 nM) and treated with or without 10 nM PGE₂. (g) cAMP levels in isolated adipocytes from WT or *Adpla* null mice treated with or without 10 nM PGE₂ (ns = not significantly different). (h) Lipolysis in isolated adipocytes treated with the EP3 antagonist L826266 (10 μM), with or without 10 nM PGE₂. Results are means ± SEM, * $P < 0.05$, ** $P < 0.01$, *** $P < 0.001$.

**Figure 5.**

Adpla deficiency prevents obesity in *ob/ob* leptin deficient mice. (a) Top panel: Representative photographs of 16 wk old male *ob/ob* and dKO mice fed a SD. Scale bar = 8 mm. Bottom panel: representative photographs of their livers and epididymal WAT. Scale bar = 6 mm. (b) Left panel: Body weights of female mice on a SD. Right panel: Food intake in 12 wk old male mice fed a SD. (c) Comparison of weights of WAT depots from WT, KO, *ob/ob* and dKO mice. (d) Carcass analysis of 40 wk old male mice fed a HFD. (e) Basal and stimulated lipolysis measured by fatty acid release from explants of epididymal WAT in 12

wk old male *ob/ob* and dKO mice fed a HFD. (f) PGE₂ and (g) cAMP levels in WAT of 12 wk old male WT, KO, *ob/ob* and dKO mice fed a HFD. Results are means ± SEM, **P* < 0.05, ***P* < 0.01, ****P* < 0.001.

Author Manuscript

Author Manuscript

Author Manuscript

Author Manuscript

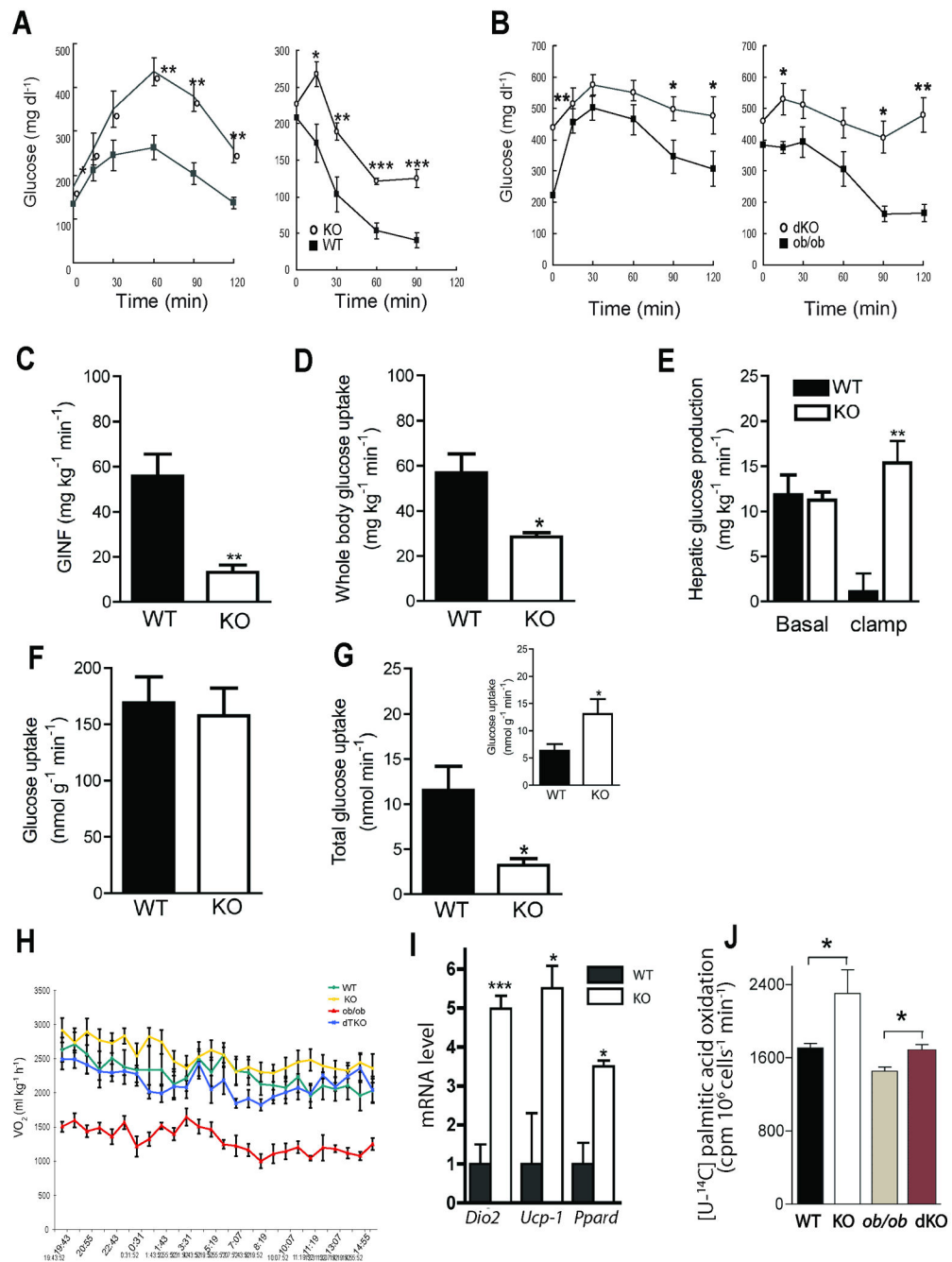


Figure 6. *Adpla* deficiency impairs glycemic control, increases energy expenditure and promotes fatty acid oxidation in WAT. (a) Glucose (GTT) and insulin (ITT) tolerance tests in 18 wk old male WT and KO mice fed a HFD (*n* = 7). (b) GTT and ITT in 14 wk old male *ob/ob* and dKO mice fed a HFD (*n* = 8–9). (c–g) Results from hyperinsulinemic euglycemic clamp performed in 12 wk old male WT and KO mice fed a HFD (*n* = 4–5). (c) Average glucose infusion rate (GINF) and (d) whole body glucose uptake. (e) Hepatic glucose production (HGP) under basal and clamp conditions. (f) Glucose uptake by skeletal muscle

(gastrocnemius). (g) Total glucose uptake and glucose uptake per gram of tissue (inset) in epididymal WAT. (h) Oxygen consumption rate (VO_2) determined via indirect calorimetry during the light (7am – 7pm) and dark (7pm – 7am) period in 18 wk old male KO and WT mice on a SD ($n = 3-6$). (i) RT-qPCR for *Ucp-1*, *Dio2* and *Ppard*, using RNA from epididymal fat from 20 wk old male WT and KO mice fed a SD ($n = 3-4$). (j) Oxidation of [U- ^{14}C]palmitate to $^{14}CO_2$ by adipocytes isolated from WT, KO, *ob/ob* and dKO mice ($n = 3$). Results are means \pm SEM, * $P < 0.05$, ** $P < 0.01$, *** $P < 0.001$.